Indian Journal of Chemistry
Vol. 61, March 2022, pp. 278-284

Hydrothermal synthesis of graphene oxide/NiO and its influence on the thermal decomposition of ammonium perchlorate

Seyed Mohammad Jebraeil & Abbas Eslami*

Department of Inorganic Chemistry, Faculty of Chemistry, University of Mazandaran, P.O.Box 47416-95447, Babolsar, Iran

*E-mail: eslami@umz.ac.ir

Received 01 December 2021; revised and accepted 17 February 2022

Graphene oxide/nickel oxide (GO/NiO) nanocomposite has been successfully synthesized through a one-step hydrothermal procedure. The GO/NiO nanocomposite is characterized by Fourier transform infrared, X-ray diffraction, scanning electron microscopy, and energy dispersive X-ray analysis. The influence of GO/NiO nanocomposites on the thermal decomposition of ammonium perchlorate (AP) is investigated by thermogravimetry, and differential scanning calorimetry analysis. The results reveal two stages thermal decomposition of pure AP changed to a one-stage highly exothermic process at much lower temperatures in the presence of GO/NiO nanocomposites. The released heat of AP thermal decomposition is increased from 649 J g^{-1} for pure AP (AP0) to 1259 and 2195 J.g^{-1}, for AP:GO/NiO 97:3 (AP3) and 95:5 (AP5) mixtures, respectively. Furthermore, decomposition temperature of AP significantly has decreased from 419 °C (AP0) to 307 °C (AP3) and 287 °C (AP5). The kinetic parameters are calculated by Kissinger equation for thermal decomposition of AP0 and AP5. The catalytic activity of GO/NiO nanocomposite is revealed by pre-exponential factor and the calculated activation energy, also the decomposition rate constant is increased from 4.2×10^{-3} s^{-1} at 419 °C (pure AP) to 1.04×10^{-2} s^{-1} at 287 °C (peak temperature of AP5 sample).

Keywords: Nanocomposite, Ammonium perchlorate decomposition, Decomposition kinetics

Graphene oxide (GO) usually occurs as a single-layer or few-layered carbon sheets. The aromatic structure of the graphene derivatives is similar to a vespiary which contains many oxygen carrying functional groups such as carbonyl, carboxyl, epoxide, hydroxyl and carboxylic acid groups on its planes and edges. GO is an interesting material because of its superior properties and optical properties and high specific surface area[1-3]. GO can be utilized as an effective support for bulk-scale production of cathodic compounds in lithium batteries, conductive polymers, and catalysts[4-6]. Such desirable catalytic activity may mostly be related to the high surface activity of GO[5].

The integration of GO and nanoparticles into nanocomposites has recently received much attention. The studies showed that the nanocomposites have enhanced catalytic activities compared to the individual single-component materials[7]. Among them, GO-supported metal oxide nanocomposites exhibit superior catalytic properties in many chemical transformations[8-10]. Nickel oxide has been applied as catalysts in organic reactions, electrode in lithium-ion battery, supercapacitor, and gas sensor[10-16]. However, NiO nanoparticles, due to their high surface, agglomerate to large cluster and cause a large decline in the specific surface area. To prevent agglomeration of NiO nanoparticles, it can be stabilized on the GO sheets. The GO sheets show unusual physical properties of two-dimensional structure such as light weight, excellent conductivity, great mechanical strength, structural flexibility, and large surface area. Therefore, the GO sheets are suitable support for transition metal oxide nanoparticles[17]. Transition metal oxides-GO hybrids have shown good catalytic activities because of high electrical and thermal conductivity and big specific surface area of GO that can be beneficial in solid propellants[18-22].

The ammonium perchlorate (AP) is an important oxidizer in solid propellant, since it has high oxygen percent (54.5% w/w), and leaves no solid residue after combustion. However, pure AP suffers from some disadvantages such as high decomposition temperatures and relatively low released heat of decomposition which occurs in a wide temperature range. Fortunately, these drawbacks can be improved by employing catalytic amounts of some additives like transition metal oxides[18-22]. Thermal decomposition of pure AP can be viewed as a three

stages process in which, at first, an endothermic phase transition takes places without mass loss at around 243 °C (orthorhombic to the cubic phase transition). Subsequently, at 300-330 °C, AP is partially decomposed with a small mass loss through an exothermic process which is known as low temperature decomposition (LTD) process. Lastly, the complete decomposition of AP which is also an exothermic process occurs at higher temperatures and is designated as high temperature decomposition (HTD) process. HTD for pure AP usually happens at temperatures above 350 °C and lead to the volatile products[18, 22]. The thermal behaviour of AP can strongly influence the burning process of propellants including of AP. So, investigation of the influence of different additives on the decomposition of AP is important[23,24].

Our previous study showed that NiO significantly increases released heat of AP decomposition, but has a smaller influence on the decreasing temperature of decomposition. It has recently been revealed that GO / metal oxide hybrids may have desirable effects on the composite propellant decomposition like AP base propellant[23,24]. So, in this work, we aim to further improve thermal decomposition of AP by means of GO-supported NiO nanoparticles so that AP decomposition occurs at fairly low temperatures with high heat release. The as-prepared composites were characterized by different techniques. The effect of GO/NiO composites on the decomposition of AP has been studied by thermogravimetric analysis (TGA) and differential scanning calorimetry (DSC) analysis. The results revealed that GO-supported NiO has excellent effects both in the rising heat release of AP decomposition and in the lowering of temperature of decomposition. Kinetic results also showed that AP decomposition is accelerated in presence of GO/NiO composites.

Experimental Details

Materials and instrumentation

The graphite powder, hydrogen peroxide (H_2O_2), sodium nitrate ($NaNO_3$), potassium permanganate ($KMnO_4$), hydrochloric acid (HCl), sulfuric acid (H_2SO_4) and nickel oxide (NiO) were bought from Merck Company, Germany. Ammonium perchlorate (NH_4ClO_4), was obtained from Fluka Company and utilized. The X-ray diffraction (XRD) patterns were recorded by a PHILIPS XRD PW1730 diffractometer with Cu Kα radiation (λ=1.54178 Å) at room temperature, and 2θ =10-80° for composition and purity analysis. Fourier-Transform infrared spectra (FT-IR) were recorded on BRUKER TENSOR 27 FTIR spectrometer using KBr pellets in the spectral range 400–4000 cm^{-1}. The morphologies of the compounds were studied by scanning electron microscopy (SEM) using TESCAN (MIRA-III) equipped with energy-dispersive X-ray spectroscopy (EDS) for semi-quantitative identification of elements. The DSC measurements were conducted with a NETZSCH DSC 214 applying with heating rate of 10 °C min^{-1} under N_2 atmosphere in a temperature range of 50–600 °C. The differential thermal analysis (DTA) and TGA were performed using a Bähr STA-504 series instrument at four heating rates (25, 20, 15 and 10 °C min^{-1}) and in Ar atmosphere in a temperature range of 50-600 °C.

Synthesis of GO

Graphene oxide (GO) was prepared with graphite powder by applying Hummers method[1,25]. In this procedure, concentrated sulfuric acid (H_2SO_4) (23 mL), sodium nitrate ($NaNO_3$) (0.5 g) and Graphite powder (1 g), were mixed in a reaction vessel and stirred at 0 °C (30 min). Next, potassium permanganate ($KMnO_4$) (3 g) were gradually added and stirred for 15 min. The obtained mixture was stirred at 35 °C (30 min). Next, 46 mL deionized water was added, and the temperature rapidly enhanced to 98 °C; then, the mixture was held at 98 °C (30 min). Then hydrogen peroxide (5 mL) and deionized water (140 mL) were added to the mixture and stirred (120 min). The colour of the suspension changed from dark brown to bright yellow in this stage. Eventually, the mixture was segregated by centrifugation, eluted successively with HCl (5%) solution, and deionized water until the pH was neutral and dried in desiccator.

Preparation of GO/NiO

After preparation of GO, in order to synthesize GO/NiO nanocomposite, GO (65 mg) was completely dispersed in deionized water (65 mL) and separately NiO (250 mg) was dissolved in deionized water and stirred for 30 min. Then these mixtures were blended and stirred for 2h. In hydrothermal treatment, the mixture shifted to the autoclave and hold at 120 °C (24 h). The obtained nanocomposite extracted with centrifugation and eluted with ethanol and deionized water, next dried.

Catalytic activity Study

The catalytic performance of NiO/GO nano-composite on decomposition of AP was investigated

by TG and DSC analysis. (AP):(GO/NiO) nanocomposite mixtures was mixed at a mass ratio of 97:3 (AP3), 95:5 (AP5) in acetone under ultrasonic waves for 1 h. Next, mixture was filtered and finally dried in an oven at 80 °C.

Results and Discussion

XRD analysis

The XRD patterns of prepared GO and GO/NiO are indicated in Fig. 1. The purity and phase crystallinity of synthesized catalyst were analysed utilizing X-ray diffraction technique. It can be seen from Fig. 1a that GO has a sharp and intense diffraction peak at 13.13° (2θ) which can be related to the (001) crystal plane of GO. After immobilization of NiO nanoparticles on GO, this peak was disappeared due to the exfoliation of GO sheets in the nanocomposite and a new peak was observed at 2θ of 19.23° which corresponds to amorphous β-$Ni(OH)_2$[26]. The XRD patterns of pure NiO were seen at (111), (200), (220), (311), and (222) crystal planes[27]. The characteristic peaks of GO/NiO nanocomposite at 2θ of 75.2°, 63.1°, 43.4°, 37.3°, and 19.32° are corresponding to (222), (311), (220), (200), (111) crystal planes of NiO, and (002) plane of GO. These peaks are related to face-centred cubic crystalline phase where peaks intensity and position are in agreement with standard spectrum (JCPDS No. 04-0835)[28]. By using the Debye-Scherrer formula as given below in Eqn. 1, the crystallite size of the prepared catalyst can be calculate:

$$d = \frac{k\lambda}{\beta \cos\theta} \quad \ldots (1)$$

Where d (nm) is crystallite size, λ (nm) is wavelength, 2θ is Bragg's, and β is full width at half maximum. The crystallite size of the NiO nanoparticles was obtained 12 nm using the Debye-Scherrer formula. Data of XRD shows that NiO nanoparticles are successfully immobilized on GO sheets.

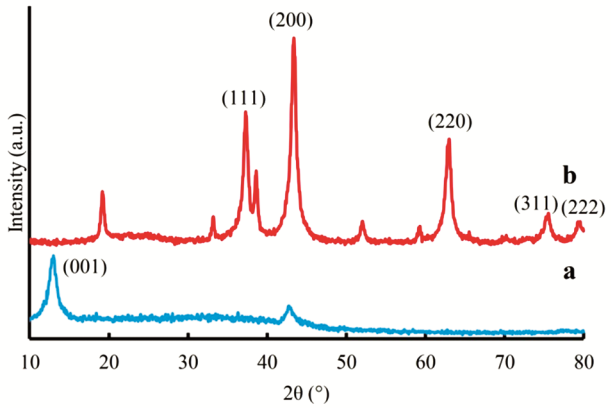

Fig. 1 — XRD patterns of (a) GO and (b) GO/NiO

FT-IR analysis

The FT-IR spectrum of the GO and GO/NiO nanocomposite is shown in Fig. 2. A band at 435 cm^{-1} shows stretching vibration of Ni-O[29]. The strong band line at 3490 cm^{-1} is related to the symmetric stretching vibration of O-H bond on surface of GO. The specific peak of GO is located at 1653 cm^{-1} is related to the C=C skeleton vibration. The vibration bands at 1218 cm^{-1} and 1710 cm^{-1} are related to the stretching vibration of C-OH and C=O in GO. The band at 3641 cm^{-1} (antisymmetric) is attributed to the OH stretching vibration of H_2O molecules adsorbed to oxygenated groups in GO. The FT-IR spectra of GO/NiO shows all bands of related to GO sheet and a band at 574 and 664 cm^{-1} related to Ni-O vibrational stretching that confirmed NiO nanoparticles were synthesized on GO sheets.

Morphology analysis

The SEM images of GO/NiO, AP/GO/NiO nanocomposites and EDS spectrum of GO/NiO nanocomposite are illustrated in Fig. 3 (a-d) and 4, respectively. As seen in Fig. 3 (a, b), the GO/NiO particles are flat in shape, and aggregated with each other, and the particles size are measured to be in the range of 20–30 nm. Fig. 3 (c,d) shows that the AP/GO/NiO sheets aggregated with each other due to van der Waals forces and inter layer hydrogen bonds between GO nanosheets[30].The EDS results revealed the presence of Ni, O and C elemental peaks that confirmed the deposition of NiO nanoparticles on GO sheets (Fig. 4).

Catalytic activity

The catalytic action of the prepared nanocomposite was investigated by DSC and TGA techniques. Fig. 5

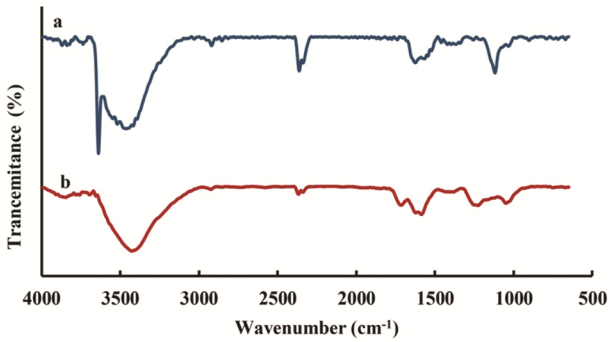

Fig. 2 — FT-IR spectra of (a) GO and (b) GO/NiO

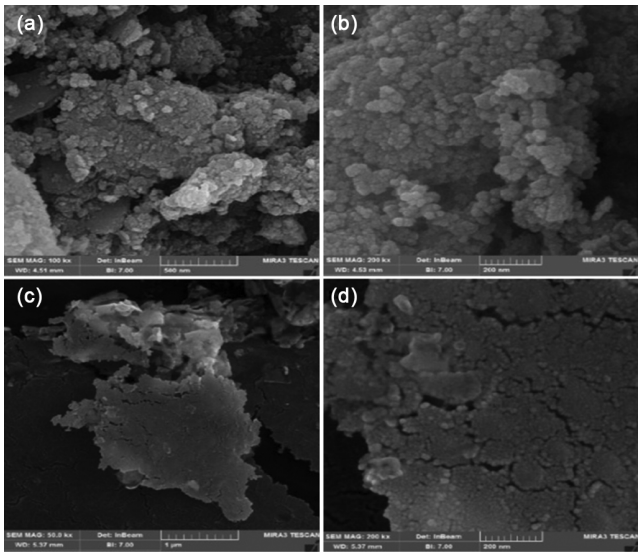

Fig. 3 — SEM images of the synthesized catalyst (GO/NiO) at (a) 200 nm, (b) 500 nm and AP/GO/NiO at 1μm (c), and 200 nm (d)

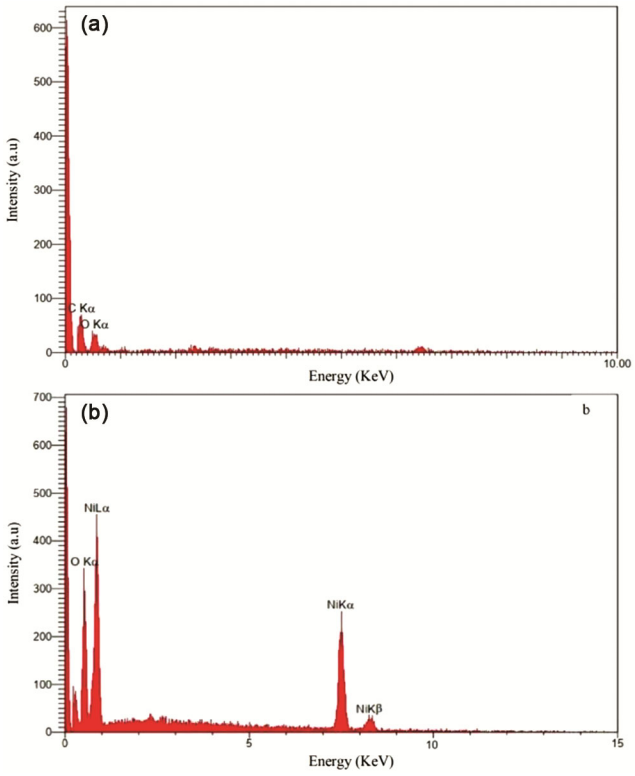

Fig. 4 — EDS spectra of (a) GO and (b) GO/NiO

shows DSC curves of AP5, and AP0. The DSC results exhibit two types of thermal events for pure AP (AP0). As mentioned earlier, the first thermal effect occurs at around 244 °C (endothermic phase transition)[31]. Then the decomposition of AP does in two consecutive stages over a relatively wide

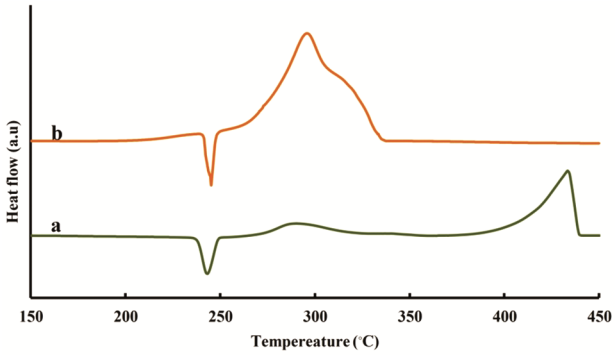

Fig. 5 — DSC curves of (a) AP0 and (b) AP5 (AP mixed with GO/NiO hybrids 5 wt%) at different heating rates

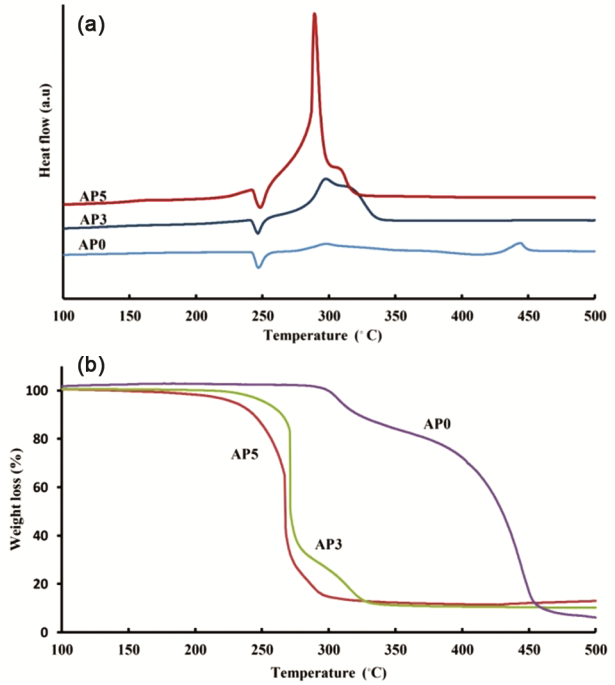

Fig. 6 — (a) DTA and (b) TGA curves of pure AP, AP mixed with GO/NiO hybrids

temperature range (250-450 °C), including LTD and HTD processes[32]. As indicated in Figs 5 and 6 (DSC and DTA/ TG curves), GO/NiO composite shows a good catalytic activity on the decomposition of AP. The catalytic activity of AP/GO/NiO nanocomposites with various weight ratios of GO/NiO to AP powders from 97:3, 95:5 (AP3, AP5,), were studied by TG measurements (Fig. 6).

The known pattern of pure AP that contains two peaks associated with LTD and HTD processes, converts to a one peak pattern in the presence of GO/NiO nanocomposite, also decomposition temperature decreases, and released energy increases. After adding catalyst to AP (95:5), the exothermic

peak of AP0 at 445 °C vanished and an exothermic peak was seen at 287 °C and the mass loss starts at a temperature near 248 °C. The results are in agreement with those of the DSC curves. The presence of GO/NiO increase the released enthalpy from ΔH= -649 J g^{-1} (AP0) to -1432 J g^{-1}. From research done to date, the mechanisms of the electron and proton transfer were proposed for HTD and LTD processes, respectively[19]. Because of the proton transfer theory at LTD, decomposition commences via proton transfer from NH_4^+ to ClO_4^- and next latter reactions cause retail decomposition of AP. According to electron transfer theory that act at HTD, electron transfer occurs from ClO_4^- to NH_4^+ and results in ClO_4° and NH_4°species (Eqn. 2)[32,33].

$$NH_4^+ + ClO_4^- \rightarrow NH_4^\circ + ClO_4^\circ \quad \ldots (2)$$

Subsequently, NH_4°could be dissociated to hydrogen atom and ammonia (Eqn. 3):

$$NH_4^\circ \rightarrow NH_3 + H \quad \ldots (3)$$

The atomic H and ClO_4 incorporate together and generate $HClO_4$, then interaction between H and $HClO_4$can be shown by the Eqn. 4:

$$HClO_4 + H \rightarrow H_2O + ClO_3^\circ \quad \ldots (4)$$

The ClO_3 radical can be transformed to the ClO_3^- ion as an electron moderator which can further react with NH_3(g) and produce volatile species like H_2O, N_2O, O_2, NO and Cl_2. However, GO in the GO/NiO nanocomposite has excellent electrical properties of n-type semiconducting behaviour[34], which makes it an electron acceptor from ClO_4. According to the usual electron transfer theory, unfilled 3d orbital in Ni^{2+}supplies may facilitate an electron transfer process. Thepositive hole in p-type semiconductor oxides (like NiO) can give electrons from AP ion and intermediate compounds, and it can improve the thermal decomposition of AP (Eqns. 5-6).

$$Ni^{2+} + ClO_4^- \rightarrow Ni^+ + ClO_4^\circ \quad \ldots (5)$$

$$Ni^+ + NH_4^+ \rightarrow Ni^{2+} + NH_4^\circ \quad \ldots (6)$$

Kinetic investigations

For thermokinetic studies of thermal decomposition of AP0 and AP5, DTA analysis has been carried out at different heating rates (20, 15, 10 and 5 °C min^{-1}). The Kissinger procedure was utilized for calculation of pre-exponential factor (A), and activation energy (E_a), due to following first-order kinetics of the decomposition of samples[32,35]. As shown in Table 1 and Fig. 7, HTD and LTD peaks of AP5 and AP0 shifted to higher temperatures by change the heating rates from 20 to 5 °C min^{-1}.

The relationship among the decomposition temperature and the heating rate can be shown by the Kissinger equation (Eqn. 7) [36]

$$\ln\frac{\beta}{T_m^2} = \ln\frac{AR}{E_a} - \frac{E_a}{RT_m} \quad \ldots (7)$$

Where, A, E_a, T_m (K), R, and β (°C min^{-1}) are pre-exponential factor, activation energy, absolute temperature of peak, gas constant, and heating rate at a given temperature, respectively. E_a for a given temperature is calculated from the slope of the

Table 1 — Effect of heating rate on the onset and maximum temperature of decomposition of AP and AP5 samples

Sample	Heating rate (°C min^{-1})	First stage (°C)		Second stage (°C)	
		Onset	Maximum	Onset	Maximum
AP					
	5	257	274	318	390
	10	267	290	334	420
	15	274	299	345	438
	20	283	307	354	442
AP5					
	5	242	244	-	-
	10	243	287	-	-
	15	243	249	-	-
	20	244	252	-	-

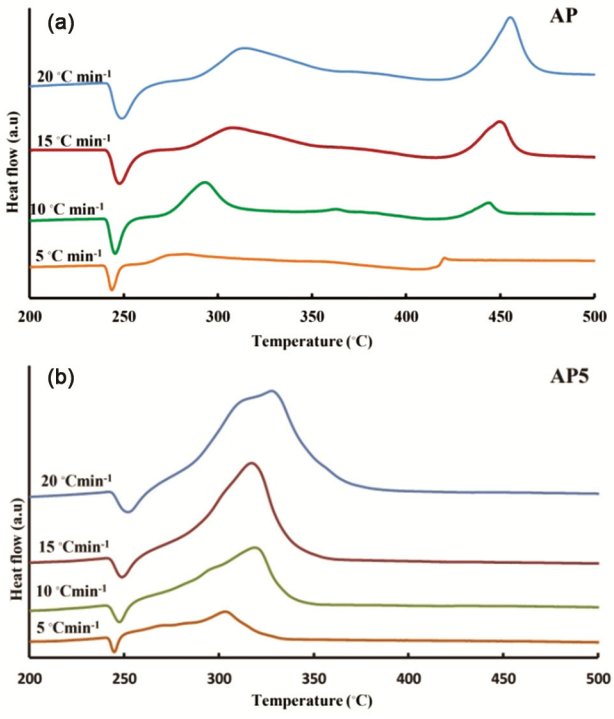

Fig. 7 — Effect of heating rate on DTA results and peak temperature of AP0 and AP5

plot $\frac{ln\beta}{T_m^2}$ versus $\frac{1}{T_m}$ linear relationship. TG analysis of AP0 and AP in presence of GO/NiO catalyst were carried out at heating rates of 20, 15, 10 and 5 °C min^{-1}. Fig. 8 shows the linear plot of $\frac{ln\beta}{T_m^2}$ versus $\frac{1}{T_m}$ for AP0 and AP5. Our kinetic calculation shows effect of nanohybrid on the rate increase of decomposition of AP i.e., an increase in lnA and/or decrease in activation energy. The calculated E_a for HTD of AP0 is about 100 kJ mol^{-1} that is in agreement with the previous reports. The E_a of decomposition of AP5 sample at HTD stage in the sample is 159 kJ mol^{-1}, and the lnA is 28. The derived kinetic parameters of first stage (LTD) and second stage (HTD) are shown in Table 2 and Fig. 7.The rate

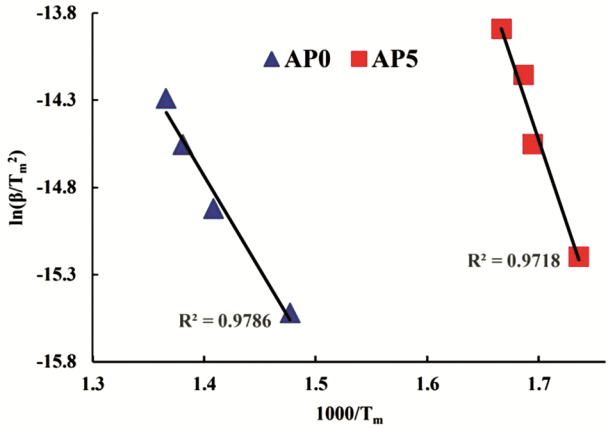

Fig. 8 — Dependence of $\ln(\beta/T^2_m)$ on $1/T_m$ of HTD for AP0 andAP5. Scattered points are experimental data, and the lines denote fitting results

Table 2 — Comparison of kinetic parameters for first and second stages of decomposition reaction of AP and AP5 by Kissinger method

sample	E_a (kJ mol^{-1})	lnA (s^{-1})	k× 10^3 (s^{-1})
AP0	100	11.4	4.2 [a]
AP5	159	28.0	10.4

[a] High decomposition temperature of blank AP

constants (k) for the reactions are calculated using Arrhenius equation as indicated in Eqn 8.

$$k=A\times e^{-\frac{E_a}{RT_m}} \quad \text{... (8)}$$

Table 2 indicates that the reaction rate constant for sample AP5 is higher than that of AP0 at temperature of peak (T_p). Whereas, the reaction rate constant for AP5 is calculated at lower temperature toward the AP0, the kinetic parameters showed that the hybrid has high catalytic influence on thermal decomposition of AP. Thermal decomposition efficiency is increased with the catalyst composition. For instance, the decomposition of AP is enhanced in the presence of GO catalyst, due to high electron mobility and high surface area of the catalyst. Moreover, another additive such as NiO can also further facilitate the electron transfer because NiO can participate in electron transfer mechanism of AP thermal decomposition through its unfilled d-orbitals. As expected, GO/NiO hybrids offer great catalytic effect in decomposition of AP.

It has been recently shown that the mixtures of GO and metal oxides may have enhanced catalytic activity for decomposition of AP. Results of some reports are showed in Table 3 and compared with catalytic activity of metal oxides in the absence of GO. The results indicates that the catalytic influence depends on the methods of preparation of the catalysts and catalyst-AP mixtures[25,37]. Therefore, it seems that GO/NiO nanocomposite have good catalytic activity with respect to previously studied catalysts such as NiO, GO/CuO, Ni/graphene. From the data given in Table 3, it can be seen that in the previous studies, HTD temperature decrease ranges from 64 °C for mixture of NiO nanoparticles with AP to 113 °C for mixture of CuO-NiO (1:1) nanoparticles with AP example[25,29,38-41]. However, results of present study revealed that GO/NiO has more pronounced effect on the decrease of HTD temperature which is about 140 °C. This study also showed that beside significant

Table 3 — Catalytic activity of different samples of NiO, CuO, GO/CuO nanoparticles on the thermal decomposition of AP

Catalyst	Catalyst/AP ratio	ΔT(°C)	HTD(°C)	Method of preparation	Ref.
GO/CuO	98:2	107	315	hydrothermal	25
NiO	94:6	69	361	green synthesis[a]	29
NiO	97:3	64	366	emulsion	38
CuO	97:3	85	345	emulsion	38
CuO-NiO	97:3	113	317	emulsion	38
CuO	98:2	89	341	chemical liquid deposition	39
NiO	99:1	93	352	biosynthetic	40
Ni/graphene	99:1	97	333	solvothermal	41
GO/NiO	95:5	140	287	hydrothermal	this work

(a): Using Aloe Vera extract

decrease of HTD temperature of AP in the presence of GO/NiO, the released heat was favorably enhanced. The released heat jumped from 450 J g^{-1} (pure AP) to 2195 J g^{-1} (AP in the presence of GO/NiO).

Conclusions

GO was successfully synthesized by using modified Hummers method then GO/NiO hybrids were synthesized by using hydrothermal procedure and characterized using FTIR, SEM, EDS, and XRD , and was applied as catalyst for decomposition of AP. The immobilization of NiO nanoparticles on GO sheet can effectively avoid aggregation of NiO particles. Therefore, the catalyst has high specific surface area and provides abundant active sites for catalytic decomposition of AP. The TG, DTA, and DSC studies indicated the released heat of AP decompositionis improved from 450 J g^{-1}(AP0) to 1259 and 2195 Jg^{-1} for AP3, AP5, respectively. The results also revealed that a significant decrease of high temperature decomposition (HTD) occurs from 419 °C for AP0 to 330 and 320 °C for AP3, and AP5, respectively.The kinetic results showed that AP thermal decomposition rate increased from 4.2×10^{-3} (pure AP, AP0) to 1.04×10^{-2} s^{-1} in the presence of catalyst(AP5). The catalytic effects of GO for AP decomposition can be attributed to its ability to provide a platform for electron transfer, which is presumed to be the main mechanism of HTD. The further enhancement of the catalytic activity in the presence of GO/NiO hybrids may be related to the synergistic effect between GO and NiO nanoparticles and can be used in the improvement of the AP-based propellants.

References

1 Hummers Jr W S & Offeman R E, *J Am Chem Soc,* 80 (1958) Article 1339.
2 Park S & Ruoff R S, *Nat Nanotechnol,* 4 (2009) 217.
3 Pei S & Cheng H-M, *Carbon*, 50 (2012) 3210.
4 Wang J, Tsuzuki T, Tang B, Hou X, Sun L & Wang X, *ACS Appl Mater Inter,* 4 (2012) 3084.
5 Wu Z S, Zhou G, Yin L C, Ren W, Li F & Cheng H M, *Nano Energy,* 1 (2012) 107.
6 Xie G, Xi P, Liu H, Chen F, Huang L, Shi Y, Hou F, Zeng Z, Shao C & Wang J, *J Mater Chem,* 22 (2012) 1033.
7 Vinothkannan M, Karthikeyan C, Kumar G G, Kim A R & Yoo D J, *Spectrochim Acta A,* 136 (2015) 256.
8 Yang X, Zhou T, Ren B, Shi Z & Hursthouse A, *J Anal Methods Chem,* 1 (2017) Article ID 3012364.
9 Abbasi S, Ahmadpoor F, Imani M & Ekrami-Kakhki M S, *Int J Environ Anal Chem,* 100 (2020) 225.
10 Jin L N, Liu Q & Sun W Y, *Chinese Chem Lett,* 24 (2013) 663.
11 Kim T W, Hwang S J, Jhung S H, Chang J S, Park H, Choi W & Choy J H, *Adv Mater,* 20 (2008) 539.
12 Li G, Wang X, Ding H & Zhang T, *RSC Adv,* 2 (2012) 13018.
13 Liu L, Li Y, Yuan S, Ge M, Ren M, Sun C & Zhou Z, *J Phys Chem C,* 114 (2010) 251.
14 Wen W, Wu J M, Lai L L, Ling G P & Cao M H, *CrystEngComm,* 14 (2012) 6565.
15 Xing W, Li F, Yan Z F & Lu G Q, *J Power Sources,* 134 (2004) 324.
16 Zhang G, Yu L, Hoster H E & Lou X W, *Nanoscale,* 5 (2013) 877.
17 Zhu Y, Murali S, Cai W, Li X, Suk J W, Potts J R & Rouff R S, *Adv Mater*, 22 (2010) 3906.
18 Bircumshaw L L & Newman B H, *Proc Math Phys,* 227 (1954) 115.
19 Boldyrev V V, *Thermochim Acta,* 443 (2006) 1.
20 Chen L, Li L & Li G, *J Alloy Compd,* 464 (2008) 532.
21 Rosser W A, Inami S H & Wise H, *Combust Flame,* 12 (1968) 427.
22 Eslami A, Hosseini S G & Bazrgary M, *J Therm Anal Calorim,* 113 (2013) 721.
23 Rajić M & Sućeska M, *J Therm Anal Calorim,* 63 (2001) 375.
24 Zhi J, Tian-Fang W, Shu-Fen L, Feng-Qi Z, Zi-Ru L, Cui-Mei Y, Yang L, Shang-Wen L & Gang-Zhui Z, *J Therm Anal Calorim,* 85 (2006) 315.
25 Fertassi M A, Alali K T, Liu Q, Li R, Liu P, Liu J, Liu L & Wang J, *RSC Adv,* 6 (2016) 74155.
26 Ahmad J, Majid K & Dar M A, *Appl Surf Sci,* 457 (2018) 417.
27 Subash V S, Alagumalai K, Chen S M, Shanmugam R & Shiuan H J, *New J Chem,* 44 (2020) 15071.
28 Wang J G, Jin L N, Qian X Y & Dong M D, *J Nanosci Nanotechnol,* 16 (2016) 8635.
29 Wu L, Wu Y, Wei H, Shi Y & Hu C, *Mater lett,* 58 (2004) 2700.
30 Chabot V, Higgins D, Yu A, Xiao X, Chen Z & Zhang J, *Energ Environ Sci,* 7 (2014) 1564.
31 Juibari N M & Eslami A, *J Therm Anal Calorim,* 136 (2019) 913.
32 Juibari N M & Eslami A, *J Therm Anal Calorim,* 130 (2017) 1327.
33 Farhadi F F, Eslami A& Kubicki M, *J Therm Anal Calorim,* 140 (2020) 1779.
34 Giovannetti G, Khomyakov P A, Brocks G, Karpan V M, van den Brink J & Kelly P J, *Phys Rev Lett,* 101 (2008) 026803.
35 Juibari N M & Eslami A, *J Therm Anal Calorim,* 128 (2017) 115.
36 Kissinger H, *Anal Chem,* 29 (1957) 1702.
37 Zhao J, Liu Z, Qin Y & Hu W, *CrystEngComm,* 16 (2014) 2001.
38 Hosseini S G & Abazari R, *RSC Adv,* 5 (2015) 96777.
39 Eslami A, Juibari N M, Hosseini S G & Abbasi M, *Cent Eur J Energ Mat,* 14 (2017).
40 Sharma J K, Srivastava P, Singh G, Akhtar M S & Ameen S, *Ceram Int,* 41 (2015) 1573.
41 Li N, Cao M, Wu Q & Hu C, *Cryst Eng Comm*, 14 (2012) 428.